Autophagy

ISSN: 1554-8627 (Print) 1554-8635 (Online) Journal homepage: www.tandfonline.com/journals/kaup20

New role for EMD (emerin), a key inner nuclear membrane protein, as an enhancer of autophagosome formation in the C16-ceramide autophagy pathway

Céline Deroyer, Anne-Françoise Rénert, Marie-Paule Merville & Marianne Fillet

To cite this article: Céline Deroyer, Anne-Françoise Rénert, Marie-Paule Merville & Marianne Fillet (2014) New role for EMD (emerin), a key inner nuclear membrane protein, as an enhancer of autophagosome formation in the C16-ceramide autophagy pathway, Autophagy, 10:7, 1229-1240, DOI: 10.4161/auto.28777

To link to this article: https://doi.org/10.4161/auto.28777

Autophagy 10:7, 1229–1240; July 2014; © 2014 Landes Bioscience

New role for EMD (emerin), a key inner nuclear membrane protein, as an enhancer of autophagosome formation in the C16-ceramide autophagy pathway

Céline Deroyer,[1] Anne-Françoise Rénert,[1] Marie-Paule Merville,[2] and Marianne Fillet[1,3,*]

[1]GIGA-R Proteomic Unit; University of Liège; Liège, Belgium; [2]Department of Clinical Chemistry; Centre Hospitalier Universitaire de Liège; Liège, Belgium; [3]Department of Analytical Pharmaceutical Chemistry; Department of Pharmacy; Centre Interfacultaire de Recherche du Médicament; University of Liège; Liège, Belgium

Keywords: autophagy, ceramide, colon cancer cells, EMD, LEM-domain, phosphorylation, PRKACA

Abbreviations: BANF1, barrier to autointegration factor 1; BCA, bicinchoninic acid; BCL2/B-cell CLL/lymphoma 2; BCLAF1, BCL-2-associated transcription factor 1; CerS, ceramide synthase; ECL, enhanced chemiluminescence; EDMD, Emery-Dreifuss muscular dystrophy; EMD, emerin; MAP1LC3B, microtubule-associated protein 1 light chain 3 beta; MAPK3, mitogen-activated protein kinase 3; HDAC3, histone deacetylase 3; λPPase, lambda protein phosphatase; MDM2, MDM2 oncogene, E3 ubiquitin protein ligase; MTOR, mechanistic target of rapamycin (serine/threonine kinase); PRKACA, protein kinase, cAMP-dependent, catalytic, alpha; SDS, sodium dodecyl sulphate

To date, precise roles of EMD (emerin) remain poorly described. In this paper, we investigated the role of EMD in the C16-ceramide autophagy pathway. Ceramides are bioactive signaling molecules acting notably in the regulation of cell growth, differentiation, or cell death. However, the mechanisms by which they mediate these pathways are not fully understood. We found that C16-ceramide induces EMD phosphorylation on its LEM domain through PRKACA. Upon ceramide treatment, phosphorylated EMD binds MAP1LC3B leading to an increase of autophagosome formation. These data suggest a new role of EMD as an enhancer of autophagosome formation in the C16-ceramide autophagy pathway in colon cancer cells.

Introduction

Ceramide is a bioactive sphingolipid, which mediates various cellular processes, including cell cycle arrest, apoptosis, senescence, and stress responses.[1-3] Although ceramide has been mainly described in the context of apoptosis,[4-7] it has also been demonstrated that it can induce other form of cell death, namely autophagy.[8,9] Autophagy is a conserved evolutionarily mechanism by which cells deliver cytoplasmic material to lysosomes through the formation of double-membrane vesicles named autophagosomes. Cytoplasmic components can be recycled to produce free amino acids and ATP that will be used for new biomolecule synthesis. Under physiological conditions the autophagic process allows cellular homeostasis. This basal level can be modified in response to different stimuli, such as amino acid deprivation, hypoxia, and chemotherapeutic drugs, or in the context of diverse diseases like cancer, diabetes, and neurodegenerative pathogenesis.[10,11] Exogenous short-chain ceramides have been notably described to induce autophagy.[12-14] For instance, Scarletti et al.[12] demonstrate that C2-ceramide can lead to an increase in autophagosome formation through the inhibition of AKT1 (v-akt murine thymoma viral oncogene homolog 1) and the upregulation of BECN1/Beclin 1. Furthermore, exogenous ceramides (C2- and C6-ceramide) have been observed to disrupt the BECN1-BCL2 (B-cell CLL/lymphoma 2) complex through the ceramide-induced phosphorylation of BCL2 causing autophagy initiation.[15] Interestingly, Spassieva et al.[16] demonstrate that downregulation of ceramide synthase 2 (CerS2) results in an increase of long-chain ceramide, including C16-ceramide, and leads to autophagy activation. More recently, it has been shown that C18-pyr-Cer treatment not only induces autophagy but also targets autolysosomes to mitochondria in HNSCC cells.[17] Nevertheless, ceramide synthase 6 (CerS6) induction, leading to C14- and C16-ceramide accumulation, has no effect on autophagy activity in this cell line.

Previously, we have demonstrated that the death-promoting factor BCLAF1 (BCL2-associated transcription factor 1) is required for the proapoptotic C16-ceramide-dependent

*Correspondence to: Marianne Fillet; Email: marianne.fillet@ulg.ac.be
Submitted: 05/01/2013; Revised: 04/01/2014; Accepted: 04/03/2014; Published Online: 05/07/2014
http://dx.doi.org/10.4161/auto.28777

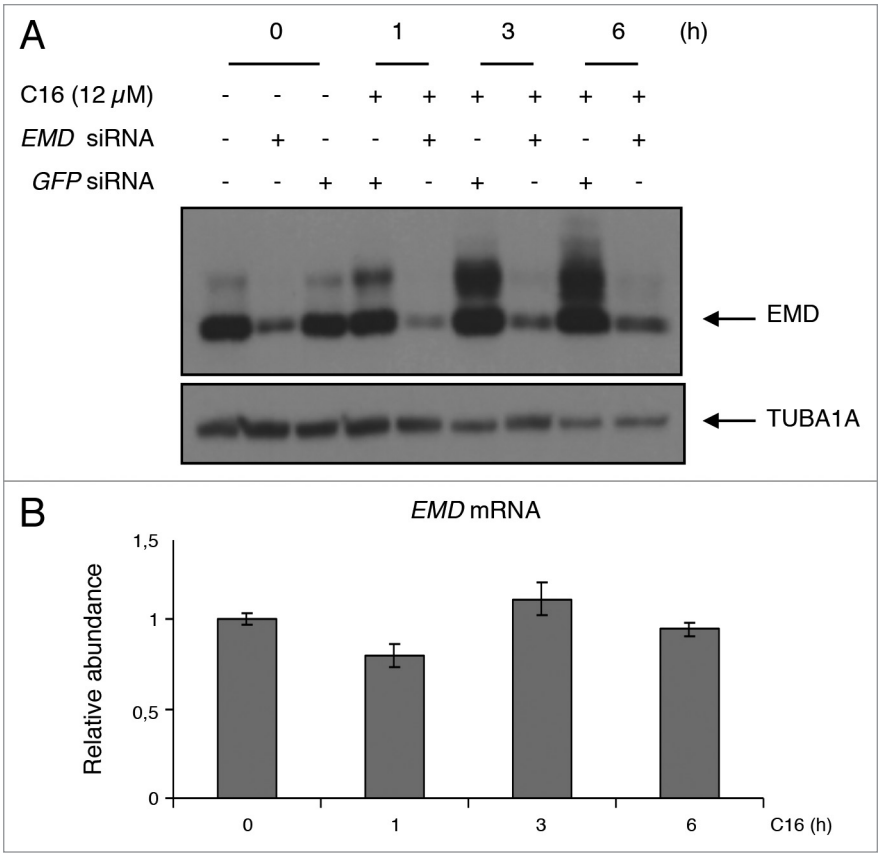

Figure 1. C16-ceramide treatment induces EMD phosphorylation. (**A**) HCT116 cells were transfected with *GFP* siRNA or *EMD* siRNA and then stimulated with C16-ceramide (12 μM) for the indicated times. EMD was revealed by western blotting using an anti-EMD antibody. An anti-TUBA1A antibody was used as an internal control. (**B**) *EMD* mRNA levels, extracted from HCT116 cells treated with and without C16-ceramide, were assessed by quantitative real-time PCR analysis.

pathway.[18] Haraguchi et al.[19] have described BCLAF1 as an EMD-binding partner. They have demonstrated that 2 mutations in EMD (S54F and delta 95 to 99), observed in Emery-Dreifuss muscular dystrophy (EDMD), disrupt BCLAF1 binding.

EMD is ubiquitously expressed and belongs to the LEM domain family of the inner nuclear membrane proteins.[20,21] This domain is essential for binding BANF1 (barrier to autointegration factor 1), a dsDNA-bridging protein, with direct roles in higher-order chromatin structure, nuclear assembly, and gene regulation.[22-28] EMD also contains a lamin-binding domain that helps to retain it in the interphase nuclear envelope.[23,28-30]

Novel EMD-associated proteins have been found by Holaska and coworkers after purification of EMD-containing complexes from HeLa cell nuclear lysates. The authors have found that each complex has distinct components involved in nuclear architecture (NMI [N-myc {and STAT} interactor], SPTAN1 [spectrin, α, non-erythrocytic 1], lamins) or in gene and chromatin regulation (BANF1, transcription regulators, HDACs).[31] More recently, it has been demonstrated that EMD binds and activates the HDAC3 (histone deacetylase 3) providing for EMD a potential role in initiating or maintaining repressed chromatin at the nuclear lamina.[32] In addition, EMD could have a role in the MAPK signaling pathway. Indeed, the MAPK3 (mitogen-activated protein kinase 3) is activated in hearts of mice with mutations in *LMNA* (lamin A/C) and *EMD* genes.[33] Consistent with this finding, Muchir et al.[34] demonstrate that reduced expression of EMD leads to MAPK3 phosphorylation in Hela and C2C12 cells.

EMD is phosphorylated in a cell cycle-dependent manner in human lymphoblastoid cells.[35] This study suggests that the phosphorylation status of EMD regulates its binding to LMNA. In accordance, Hirano et al.[36] show that EMD is phosphorylated at the M-phase in a *Xenopus* egg cell-free system on 5 specific residues, 4 serine and 1 threonine residues: Ser49, Ser66, Thr67, Ser120, and Ser175. The authors demonstrate that phosphorylation on Ser175 is responsible for the dissociation of EMD from BANF1. A study of Roberts et al.[37] demonstrates that, PRKACA (protein kinase, cAMP-dependent, catalytic, α) phosphorylates EMD on Ser49. EMD can also be phosphorylated on tyrosine residues.[38,39] By a proteomic approach, Schlosser et al.[40] have identified 3 tyrosine-phosphorylation sites in mouse EMD and 5 in human EMD. In accordance, Tifft et al.[41] have identified 3 tyrosine kinases, which phosphorylate directly EMD (ERBB2/HER2, SRC and ABL). They also show that both LEM domain and distal phosphorylatable tyrosine residues are involved in the binding of EMD to BANF1. Moreover, PTPN1 (protein tyrosine phosphatase, nonreceptor type 1), a sumoylated protein tyrosine phosphatase, has been identified to regulate the tyrosine phosphorylation status of EMD in a cell-cycle-dependent manner.[42]

To our knowledge, EMD had never been studied in the context of the ceramide signaling pathway. Here, we investigated the regulation of EMD expression and post-translational modifications induced by C16-ceramide in colon adenocarcinoma cells (HCT116). We explored whether EMD could be involved in the apoptotic, cell-cycle, and autophagic C16-ceramide-dependent pathway.

Results

C16-ceramide treatment induces *EMD* phosphorylation

The expression of EMD was found to increase after stimulation of HCT116 cells by C16-ceramide (**Fig. 1A**). After ceramide treatment, slower-migrating bands could also be observed. The expression of the EMD upper band increased in a time-dependent manner and disappeared with the transfection of an *EMD*

siRNA, suggesting a post-translational modification. Moreover, the *EMD* mRNA levels in HCT116 treated with or without C16-ceramide remained unchanged (**Fig. 1B**).

As described in the introduction, EMD is phosphorylated in a cycle-dependent manner.[35,36] Therefore we investigated whether the modifications were reversible by phosphatase treatment (λPPase at 30 °C for 30 min). As can be seen in **Figure 2A**, incubation with phosphatase caused loss of the upper EMD bands.

As several kinases were described to be implicated in EMD phosphorylation,[37,41,43,44] we examined the effect of staurosporine, a broad-spectrum kinase inhibitor. The cells were pretreated 30 min before C16-ceramide treatment for 1, 3 or 6 h. As can be seen in **Figure 2B**, 100 mM of staurosporine reduced significantly EMD phosphorylation induced by C16-ceramide treatment. A study of Roberts et al.[37] demonstrates that EMD was phosphorylated during interphase by PRKACA. To verify if PRKACA phosphorylates EMD in our model, cells were pretreated with the PRKACA inhibitor H89 (5 μM, 1 h) and stimulated for 1, 3, or 6 h with C16-ceramide. As shown in **Figure 2C**, H89 reduced EMD phosphorylation at 1 and 3 h of ceramide treatment. This result indicates that PRKACA is involved in the EMD phosphorylation triggered by C16-ceramide. To confirm the implication of PRKACA in the ceramide-mediated EMD phosphorylation, we investigated other PRKACA inhibitors and a PRKACA activator. The inhibition of PRKACA with a protein kinase inhibitor (PKI 14-22 amide, myristoylated, which acts on the catalytic site) prevented the phosphorylation of EMD, which strengthens the hypothesis that PRKACA could be the kinase involved in the C16-ceramide-induced EMD phosphorylation (**Fig. S1A**). The use of Rp-8-Br-cAMP, an analog of cAMP that inhibits PRKACA, induced a slight decrease of EMD phosphorylation compared with treatment with C16-ceramide alone (**Fig. S1B**). This demonstrates that the type I of PRKACA is involved in EMD-phosphorylation upon ceramide treatment. Finally, HCT116 cells were pretreated with 8-CPT-cAMP, a PRKACA activator. In control cells (without ceramide stimulation), we observed an induction of EMD phosphorylation. The same result was obtained after C16-ceramide stimulation for 3 h (**Fig. S1C**). These data support the hypothesis that C16-ceramide treatment induces EMD phosphorylation through the PRKACA.

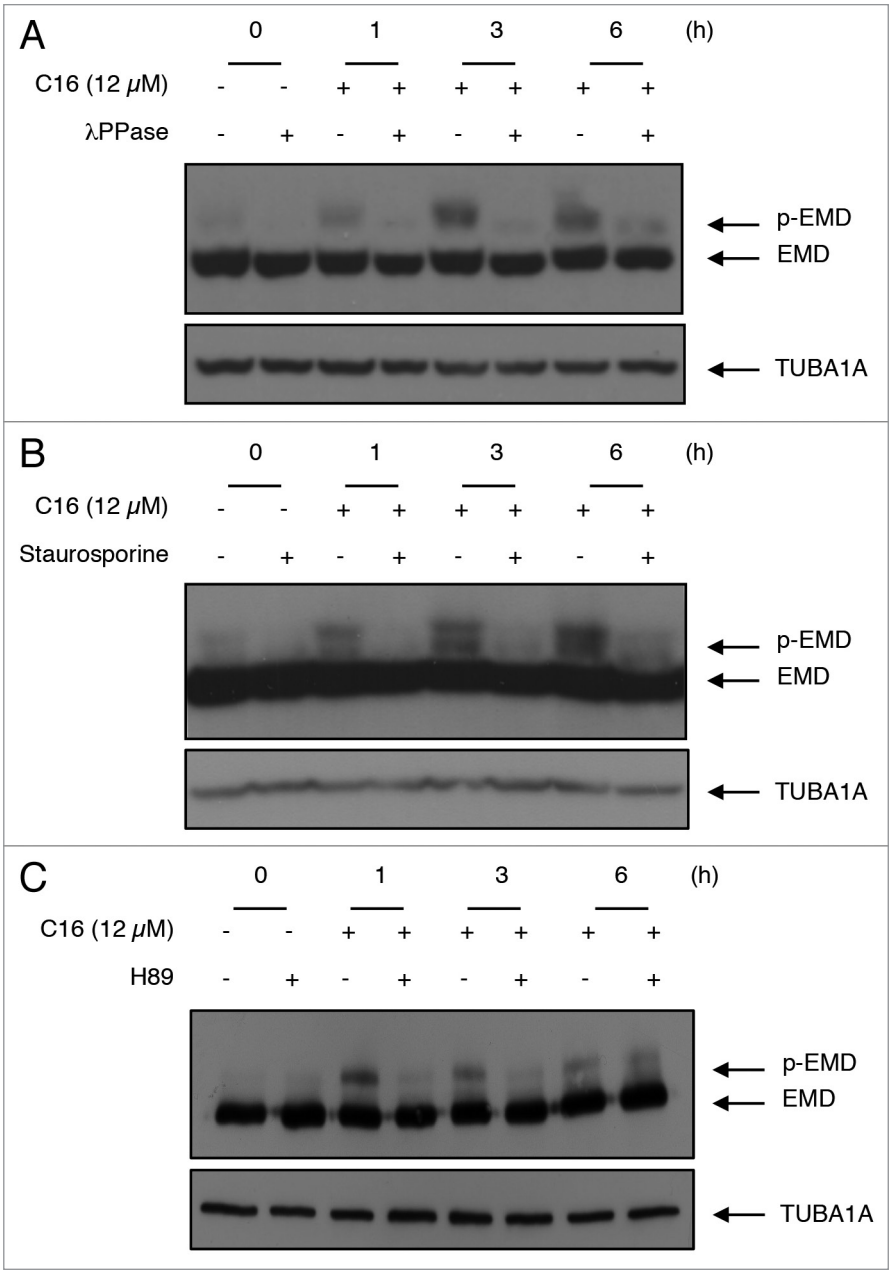

Figure 2. Phosphatase (λPPase), general kinase inhibitor (staurosporine), and PRKACA inhibitor (H89) reverse EMD modification. (**A**) Colon cancer cells were treated with or without C16-ceramide for 1, 3, and 6 h. Protein extracts were incubated in the absence or presence of alkaline phosphatase (λPPase) at 30 °C for 30 min. Protein extracts were separated on SDS polyacrylamide gel and immunoblotting was revealed with anti-EMD and anti-TUBA1A antibodies. (**B**) HCT116 cells were pretreated with staurosporine (100 nM) for 30 min and left untreated or stimulated with C16-ceramide (12 μM) for 1, 3, and 6 h. Western blotting analysis was performed using an anti-EMD and an anti-TUBA1A antibody. (**C**) HCT116 were pretreated with the PRKACA inhibitor, H89 (5 μM) for 1 h and treated with or without C16-ceramide for the indicated periods of time. Cell extracts were subjected to anti-EMD and anti-TUBA1A antibodies for western blot analysis.

In order to know if EMD can be phosphorylated upon other ceramide treatment and in other cell lines, HCT116, HT29, and

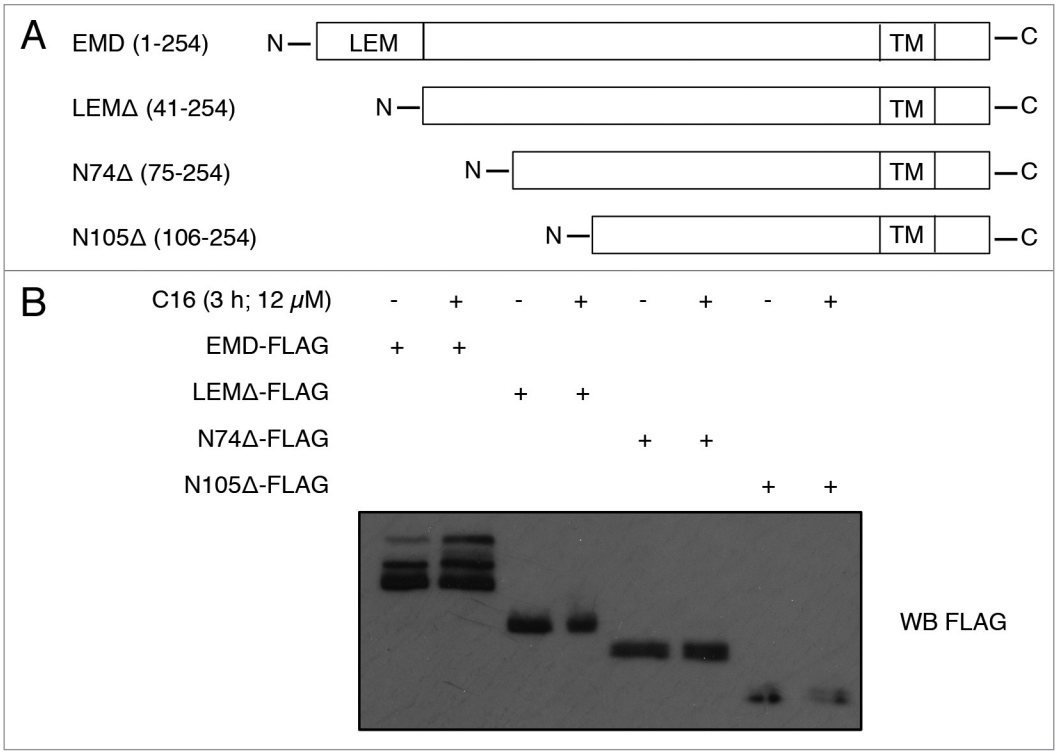

Figure 3. C16-ceramide induces EMD phosphorylation on its LEM domain. (**A**) Schematic representation of full-length EMD and mutants (LEMΔ, N74Δ, N105Δ). (**B**) HCT116 cells were transfected with EMD-FLAG, LEMΔ-FLAG, N74Δ-FLAG, N105Δ-FLAG, or empty vector and subjected to C16-ceramide for 3 h. Cell extracts were analyzed with an anti-FLAG western blot.

HEK293 cells were stimulated with the short-chain ceramides C2 and C8 and with the long-chain ceramides C16 and C18. As control, the inactive ceramide analog C2-dihydroceramide (C2-DHC) was used. It appeared that EMD is phosphorylated upon C2-, C8-, C16-, and C18-ceramide treatment but not C2-DHC in the 3 cell lines (**Fig. S2**). This demonstrates that EMD phosphorylation occurs in different cell lines and is triggered by short- and long-chain ceramides. Conversely, the inactive ceramide analog, C2-DHC, is not able to do so.

To determine which EMD domains are phosphorylated by C16-ceramide, we generated a variety of EMD mutants tagged with FLAG lacking N-terminal amino acids (LEMΔ, N74Δ, and N105Δ, **Fig. 3A**). Both full-length EMD and mutants were transfected and cells were treated with C16-ceramide for 3 h. Western blot analysis of FLAG showed that all the EMD mutants had lost the phosphorylation induced by ceramide compared with the full-length EMD (**Fig. 3B**). This result suggests that C16-ceramide induces EMD phosphorylation on its LEM domain.

EMD is not involved in C16-ceramide apoptosis and cell cycle signaling pathways

We have previously reported that C16-ceramide induces apoptosis in HCT116 cells and that BCLAF1 could be an intermediate in this pathway.[18] We showed that BCLAF1 negatively regulated *MDM2* (MDM2 oncogene, E3 ubiquitin protein ligase) gene expression in response to C16-ceramide stimulation in HCT116 cells. In order to investigate if EMD could have a role in ceramide-induced apoptosis in colon cancer cells, cells were depleted using an *EMD* siRNA (or a *GFP* siRNA as control) and then treated with or without C16-ceramide. We observed that EMD depletion did not affect cell viability and activities of CASP3 or CASP7 (caspases 3 or 7) (**Fig. S3B and S3C**). To find out if the phosphorylation of EMD is involved in the decrease of cell viability triggered by C16-ceramide, a viability test was performed with cells expressing WT EMD and the nonphosphorylatable mutant LEMΔ EMD. Cells were treated with or without C16-ceramide for 1, 3, and 6 h. Cells expressing WT EMD were also pretreated with H89 in order to inhibit the phosphorylation of EMD induced by ceramide. We observed that the inhibition of EMD phosphorylation triggered by C16-ceramide did not affect cell viability (**Fig. S3D**).

Moreover, ceramide is also known to induce cell cycle arrest.[45] We thus measured the expression of p-RB1 (retinoblastoma 1) and CCND1 (cyclin D1), 2 proteins known as cell cycle activators. Upon C16-ceramide treatment, the level of these 2 proteins significantly decreased (**Fig. S4A**). Flow cytometry analysis also pointed out a decrease in the quantity of cells in S and G_2 phases after 16 h C16-treatment (**Fig. S4B**). Finally, to determine the potential implication of EMD, flow cytometry analysis was performed after depletion or overexpression of EMD followed by ceramide treatment. No effect of EMD on the percentage of cells in phase S and G_2 was observed (**Fig. S4C and S4D**).

EMD enhances the C16-ceramide autophagic pathway

Short-chain ceramides have been described to induce autophagy.[12,13,15,46] Moreover, downregulation of CerS2 inducing

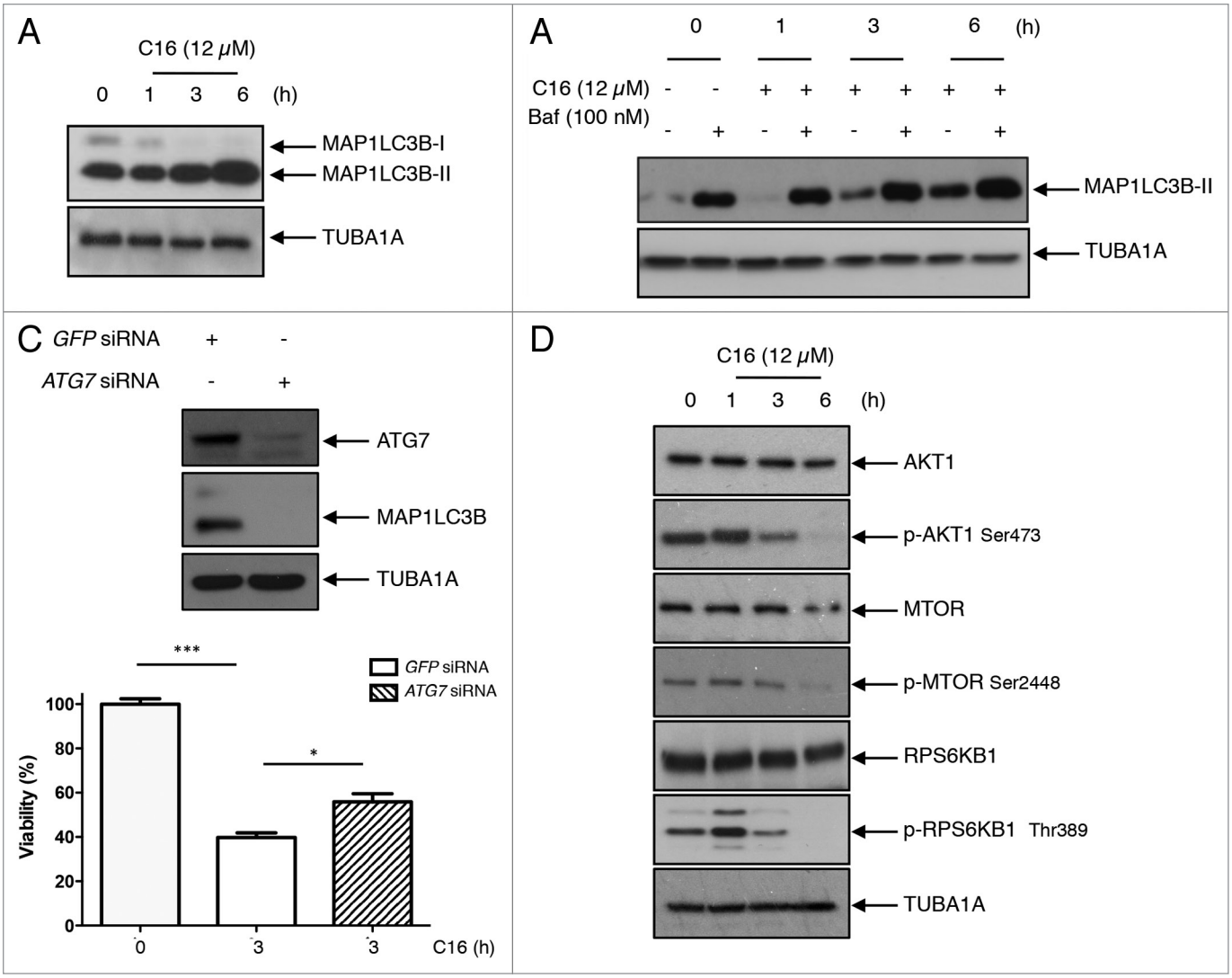

Figure 4. C16-ceramide treatment induces lethal autophagy in HCT116 cells. (**A**) HCT116 were treated with C16-ceramide for the indicated periods of time. Cell lysates were analyzed by immunoblotting with anti-MAP1LC3B and -TUBA1A antibodies. (**B**) HCT116 were pretreated with bafilomycin A_1 (100 nM) for 3 h and treated with or without C16-ceramide. Cell lysates were analyzed by immunoblotting with anti-MAP1LC3B and -TUBA1A antibodies. (**C**) HCT116 cells were transfected with *GFP* siRNA or *ATG7* siRNA. ATG7 and MAP1LC3B were revealed by western blotting using anti-ATG7 and anti-MAP1LC3B antibodies. The anti-TUBA1A antibody was used to detect TUBA1A as an internal control (top). Viability test. HCT116 cells were transfected with *GFP* siRNA or *ATG7* siRNA and then treated with and without C16-ceramide for 3 h. Cell viability was measured using the WST1 assay (bottom). (**D**) Cells were treated with or without C16-ceramide and cell lysates were analyzed with anti-AKT1, -pAKT1, -MTOR, -pMTOR, -RPS6KB1, -pRPS6KB1, and -TUBA1A antibodies.

autophagy is also associated with a significant increase of C14- and C16-ceramides levels.[16] Recently, Sentelle et al.[17] have shown that C18-ceramide directly mediates autophagy. Activation of autophagy triggered by C16-ceramide in our model was thus investigated by studying MAP1LC3B-II/microtubule-associated protein 1 light chain 3 β-II turnover, which correlates with autophagosome accumulation.[47] HCT116 cells were treated with ceramide for 1, 3, and 6 h. As shown in **Figure 4A**, the MAP1LC3B-II level increased in a time-dependent manner whereas the MAP1LC3B-I level decreased. Because an increase of MAP1LC3B-II expression can be due to an inhibition of the autophagosomes clearance as well as to an increase of their formation, we prevented the lysosomal degradation before ceramide treatment with bafilomycin A_1. In those conditions, MAP1LC3B-II level increased upon ceramide treatment showing that C16-ceramide leads to a complete autophagic process (**Fig. 4B**). To confirm the induction of autophagy by ceramides, 3 different cell lines (HCT116, HT29, and HEK293) were treated with short-chain ceramides C2 and C8 and long-chain ceramides C16 and C18. As a negative control, the inactive ceramide analog C2-dihydroceramide (C2-DHC) was used. MAP1LC3B-II expression was increased after C2-, C8-, C16-, and C18-ceramide treatment but not C2-DHC in the 3 cell lines. This demonstrates that autophagy induction occurs in different cell lines and is triggered by short- and long-chain ceramides (**Fig. S5**).

As we have shown in **Figure S3**, C16-ceramide induces a decrease in cell viability partly due to apoptosis. To know if C16-ceramide-mediated autophagy also contributes to cell death, the molecular machinery of autophagy was blocked using a siRNA against the *ATG7* (autophagy-related 7) gene. The transfection of an *ATG7* siRNA induced a significant decrease of ATG7 protein expression as well as MAP1LC3B protein expression (**Fig. 4C**, top). A viability test was performed and showed that the inhibition of autophagy prevented cell death in response to C16-ceramide treatment compared with si*GFP*-transfected cells (**Fig. 4C**, bottom). This demonstrates that autophagy mediated by C16-ceramide contributes to cell death.

Many signaling pathways lead to autophagy; most studied are the MTOR (mechanistic target of rapamycin [serine/threonine kinase]), the AKT1 and the MAPK (mitogen-activated protein kinase) i.e. MAPK1, MAPK3, MPAK8, and MAPK14 pathways. In our model, cells treated with C16-ceramide showed that the expression level of AKT1, MTOR, and RPS6KB1 (ribosomal protein S6 kinase, 70 kDa, polypeptide 1) remained constant while the phosphorylation level of AKT1 on Ser473, MTOR on Ser2448, and RPS6KB1 on Thr389 decreased after 3 and 6 h of C16-ceramide treatment (**Fig. 4D**). Furthermore, the phosphorylation levels of MAPK14, MAPK1, MAPK3, and MAPK8, other proteins implicated in autophagy activation, remained constant (data not shown).

To study the implication of EMD in autophagy activation triggered by ceramide, cells were transfected with EMD-FLAG vector (or with empty vector as control) and then subjected to C16-ceramide treatment. As shown in **Figure 5A**, EMD overexpression had nearly no effect on MAP1LC3B-II level expression in untreated cells. On the contrary, after ceramide treatment, MAP1LC3B-II level increased upon EMD overexpression, especially after 3 h of treatment. Moreover, knockdown of EMD using a specific siRNA led to a decrease in the MAP1LC3B-II expression after 6 h of C16-ceramide treatment (**Fig. 5B**). The autophagosomes accumulation was then visualized using immunofluorescence by labeling MAP1LC3B. In untreated cells, almost no MAP1LC3B was detected. Punctated structures were visualized after 3 h of ceramide treatment indicating the formation of autophagosomes (**Fig. 5C**, left). The percentage of cells presenting a punctated MAP1LC3B was significantly higher (30%) upon ceramide treatment compared with untreated cells (**Fig. 5C**, right). In untreated cells, the overexpression of EMD led to a slight increase of punctated cells (4%). Moreover, the number of fluorescent cells increased more (22%) in EMD overexpressed cells after 3h of ceramide treatment compared with control cells (**Fig. 5C**).

***EMD* binds directly to MAP1LC3B upon ceramide treatment**

To verify whether EMD could interact with MAP1LC3B, an EMD-FLAG immunoprecipitation was performed. Western blotting analysis of the anti-FLAG immunoprecipitates with an anti-MAP1LC3B antibody showed the binding of MAP1LC3B with EMD in ceramide-treated cells (**Fig. 6A**). In order to know if EMD interracts directly with MAP1LC3B, an endogenous coimmunofluorescence analysis was performed upon C16-ceramide treatment. In untreated cells, a few particles corresponding to MAP1LC3B were present and no colocalization was detected with EMD (**Fig. 6B**, top). After C16-ceramide treatment, punctated structures corresponding to autophagosomes formation appeared (**Fig. 6B**, bottom). MAP1LC3B punctated structures were bonded to the nucleus and colocalized partially with EMD. This demonstrated that endogenous EMD could bind directly to endogenous MAP1LC3B upon C16-ceramide treatment.

The phosphorylation of EMD is required for autophagy induction

Since we have shown that ceramide induces EMD phosphorylation and that EMD overexpression increases the autophagic activity in ceramide-treated cells, we investigated whether the phosphorylation of EMD is responsible of the autophagy induction. Cells were thus pretreated with H89, an inhibitor of PRKACA, which is responsible of the EMD phosphorylation (see **Fig. 2C**), and then treated with C16-ceramide. In those conditions, the MAP1LC3B-II level appeared decreased in H89-pretreated cells compared with control cells (**Fig. 7A**). Considering that the phosphorylation of EMD occurs on its LEM-domain, we also compared the MAP1LC3B-II expression level after transfection of both the full-length and LEMΔ EMD vector. The expression level of MAP1LC3B-II was found decreased in cells transfected with the LEMΔ vector in comparison to the full-length vector upon ceramide treatment (**Fig. 7B**).

Discussion

In addition to its role in assembly and maintenance of nuclear-lamina structure, other functions have been proposed for EMD such as its implication in the regulation of gene expression and in the MAPK.[19,28,34,48,49] It is also known that EMD is phosphorylated in a cell cycle-dependent manner in vivo during all phases of the cell cycle, but the greatest degree of phosphorylation is observed in the M phase.[35]

In this study, we demonstrated that C16-ceramide induces the expression of several EMD forms (**Fig. 1A**). It is noteworthy that these modifications are reversible by treatment with phosphatase and reduced by treatment with the kinase inhibitor, staurosporine (**Fig. 2A and B**), which indicates that C16-ceramide induces EMD phosphorylation. Furthermore, we have shown that C16-ceramide is also able to induce EMD phosphorylation in other cell lines and that C2-, C8- and C18-ceramide act in the same manner (**Fig. S2**).

It is likely that a hyperphosphorylation of EMD was present after 3 and 6 h of C16-ceramide treatment (**Fig. 1A**) and thus we can hypothesize that EMD exhibits multiple phosphorylation sites. Indeed, 68 serine, tyrosine, or threonine residues are present in the EMD amino acids sequence and, among them, 18 residues have already been identified to be phosphorylated in different cell lines.[36,40,50,51] In this study, we demonstrated that C16-ceramide induces phosphorylation of EMD on its LEM domain (**Fig. 3B**). This domain contains 10 phosphorylatable

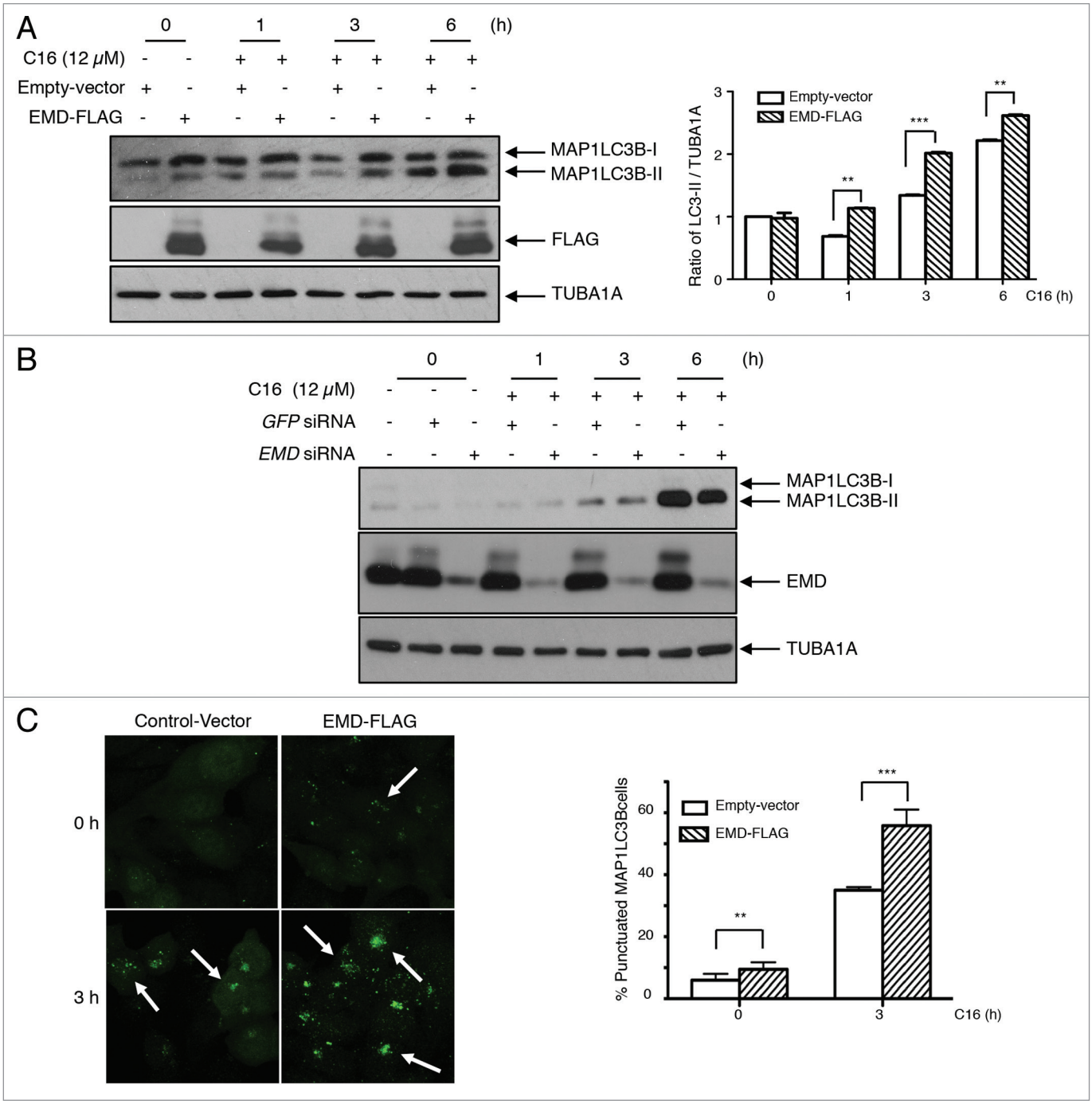

Figure 5. Implication of EMD in the C16-ceramide autophagic pathway (**A**) HCT116 cells were transfected with EMD-FLAG or empty vector and then left untreated or stimulated with C16-ceramide for the indicated times. Cell extracts were assayed using anti-MAP1LC3B, -EMD and -TUBA1A antibodies for western blotting analysis (left). The intensity of each band corresponding to MAP1LC3B-II was measured with the Quantity One software (Bio-Rad). Data are representative of 3 independent experiments and *P* values were calculated using *t* tests (**P* < 0.05; ***P* < 0.001; ****P* < 0.0001) (right). (**B**) HCT116 cells were transfected with *GFP* siRNA or *EMD* siRNA and then stimulated with C16-ceramide (12 μM) for the indicated times. MAP1LC3B was revealed by western blotting using an anti-MAP1LC3B antibody. Anti-EMD and anti-TUBA1A antibodies were also used. (**C**) Cells of each condition were stained with anti-MAP1LC3B antibodies and analyzed with confocal microscopy. Representative fluorescent images (left). Statistic results of the percentage of cells presenting a punctate distribution of MAP1LC3B (right).

residues and at least 3 tyrosines (Tyr4, Tyr19, and Tyr41) are phosphorylated in vivo.[52] The phosphorylation of this LEM-domain at these tyrosine residues plays an important role in the regulation of EMD binding to BANF1.[41]

Furthermore, our results indicate that PRKACA is implicated in C16-ceramide induced-EMD phosphorylation (**Fig. 2C**; **Fig. S1**); but H89, a PRKACA inhibitor, did not inhibit completely its phosphorylation, suggesting that PRKACA is not the

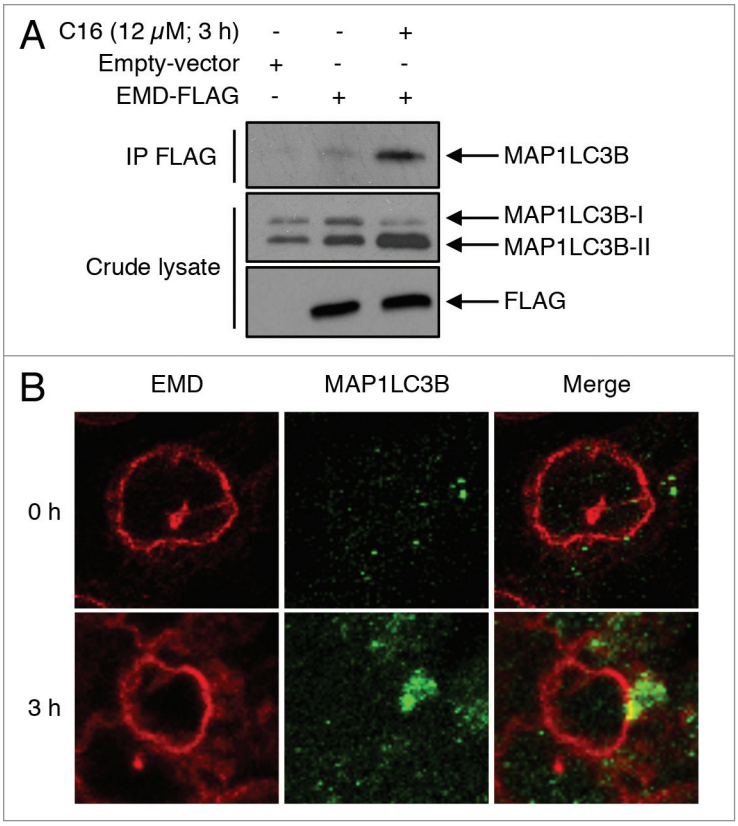

Figure 6. EMD binds MAP1LC3B upon ceramide treatment. (**A**) Cells were transfected with EMD-FLAG or with empty vector and then treated with or without C16-ceramide for 3 h. After immunoprecipitation of FLAG, MAP1LC3B was revealed by western blotting using an anti-MAP1LC3B antibody. (**B**) Representative fluorescent images of HCT116 cells untreated or treated with C16-ceramide for 3 h and stained with both anti-EMD and -MAP1LC3B antibodies. Cells were analyzed with confocal microscopy.

only kinase involved. Therefore, addressing the identification of all the phosphorylated EMD residues and their related kinases remains important to go further in the understanding of the EMD phosphorylation mechanism triggered by ceramide.

It is established that the use of exogenous ceramide analogs as therapeutic agents can promote apoptotic pathways in cancer cells.[5,53,54] Moreover, as reviewed by Levy and Thorburn,[55] many cancer therapies also induce autophagy within tumor cells. Cancer cells activate autophagy in response to chemotherapeutic stress as a defense mechanism and can both promote or inhibit cancer cells drug resistance.[56,57] However, the underlying mechanism is not well understood. Several clinical trials evaluating autophagy are underway. For example, in rectal and colon adenocarcinoma, hydrochloroquin is used in combination with chemotherapy agents to block autophagy inducing tumor cells death.[58] Oppositely, in the same cancers, cetuximab stimulates autophagy killing cancer cells.[59]

In this context, ceramide has been highlighted to play an important role in autophagy induction.[60-62] Effectively, chemotherapeutic drugs such as daunorubicin or vincristine increase intracellular ceramide generation.[63,64] Moreover, sorafenib induces autophagy only when intracellular ceramide levels are increased.[60] In glioma cells, endoplasmic reticulum stress and ceramide production are induced by IL24/melanoma differentiation association protein 7 therapy leading to cell autophagy and death.[61] All these studies show the importance of a better understanding of the complex network of sphingolipid signaling in cancer therapy as well as in the autophagy pathway.

Several signaling pathways have already been identified to be involved in autophagy activation triggered by ceramide.[12,13,15,60] Guenther et al.[65] have reported that ceramide acts in a similar manner to amino acid deprivation, inducing the inhibition of MTOR. This is demonstrated by the inhibition of its direct substrate, RPS6KB1. In accordance, we found that C16-ceramide inactivated the AKT1-MTOR pathway in HCT116 cells leading to autophagy induction. Indeed, upon ceramide treatment, we noticed a decrease in the phosphorylation of AKT1 on Ser473, of MTOR on Ser2448 and of its direct substrate RPS6KB1on Thr389 (**Fig. 4D**), which subsequently leads to MAP1LC3B lipidation (**Fig. 4A**). It is noteworthy that autophagy activation is not exclusively induced by C16-ceramide and in HCT116 cells. Indeed, as shown in **Figure S5**, C2-, C6-, and C18-ceramides also induced MAP1LC3B lipidation in HCT116 and other cell lines. This is consistent with the finding of Sentelle et al.[17] showing that C16- and C18-pyridinium-ceramides produce similar effects on the induction of autophagy. Note, however, that exogenous ceramide has been used to induce autophagy. It could be interesting to verify in a future study if the generation of endogenous ceramide by overexpression of CERS5/ceramide synthase 5 or CERS6 would have the same effect.

We then brought out the implication of EMD in this process. Indeed, EMD overexpression enhanced MAP1LC3B-II expression upon ceramide, especially after 3 h of treatment (**Fig. 5A**) and EMD depletion leads to a decrease of MAP1LC3B-II expression after 6 h of C16-ceramide (**Fig. 5B**). By immunofluorescence, we pointed out that the number of autophagosomes was increased by 4% after EMD overexpression, compared with control, in untreated cells and by 22% in C16-ceramide-treated cells (**Fig. 5C**). Furthermore, we showed that EMD could act directly on autophagosome formation through its binding with MAP1LC3B upon ceramide treatment (**Fig. 6A**). Moreover, the immunofluorescence analysis demonstrated that endogenous MAP1LC3B nearest the nucleus colocalized with endogenous EMD when cells are stimulated with ceramide (**Fig. 6B**). This demonstrated that EMD induces autophagy through its direct interaction to MAP1LC3B-II upon ceramide treatment. In this context, Sentelle et al.[17] have shown that the interaction of C18-Pyr-cer to MAP1LC3B-II is responsible for lethal autophagy mediated by ceramide. Therefore, it could be interesting to investigate in a future work whether the same mechanism is playing a role in our model and if C16-ceramide could be part of the EMD-MAP1LC3B-II complex.

Finally, our results suggest that EMD could enhance the autophagy activity through its phosphorylation triggered by

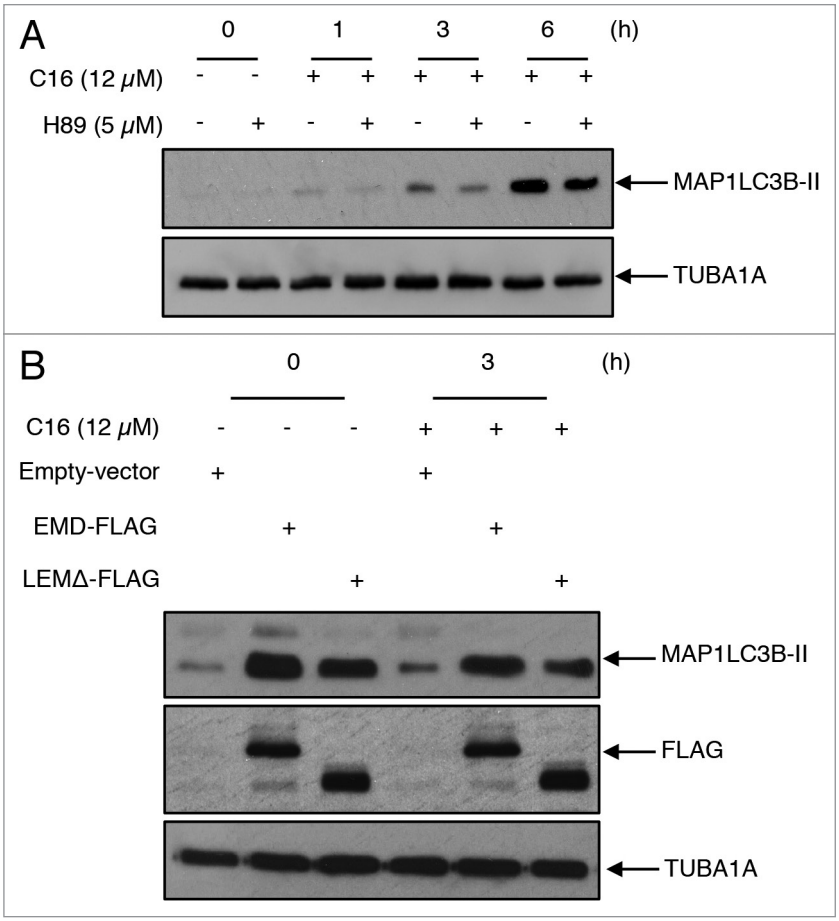

Figure 7. EMD induces autophagosome formation through its phosphorylation triggered by C16-ceramide (**A**) HCT116 were transfected with EMD-FLAG vector or with empty vector. Cells were then pretreated with the PRKACA inhibitor, H89 (5 μM) for 1 h and treated with or without C16-ceramide for 1, 3, or 6 h. Cell lysates were analyzed by western blotting using an anti-MAP1LC3B antibody. (**B**) Cells were transfected with EMD-FLAG, LEMΔ-FLAG, or empty-vector and then treated with ceramide for 3 h. MAP1LC3B, FLAG and TUBA1A were revealed by western blotting using anti-MAP1LC3B, anti-FLAG, and anti-TUBA1A antibodies.

ceramide. Indeed, transfection of the non-phosphorylatable mutant LEMΔ vector failed to increase the MAP1LC3B-II level, as well as does the wild-type EMD vector (**Fig. 7B**). Also, the inhibition of PRKACA, the kinase responsible for EMD phosphorylation, led to a decrease of the MAP1LC3B-II expression (**Fig. 7A**).

Although it was never shown that EMD has a role in autophagy activity, Park et al.[66] show, in the context of nuclear envelopathies, that autophagosomes are detected near the nucleus. It has been observed that the MAP1LC3B-signal is stronger at the area where lamins and EMD are detected suggesting an interaction between these proteins. These results are consistent with our finding and support the idea that EMD could have a role in autophagy regulation and more specifically on autophagosome formation.

In this work, we underscored a new role for EMD as an inducer of autophagy after the phosphorylation of its LEM-domain triggered by C16-ceramide. This study provides new foundations for understanding the ceramide autophagic signaling pathway and offers new insights in the development of novel therapeutic strategies.

Materials and Methods

Cell culture, biological reagents, and treatments

HCT116 human colon carcinoma cells (ATCC, CCL-247) were cultured in McCoy's 5A modified medium (Lonza, 12-688F) supplemented with 10% fetal bovine serum (Sigma, F7524), 1% L-glutamine (200 mM) (Lonza, 17-605E), 100 units/ml penicillin and 100 μg/mL streptomycin (Lonza, 17-602E). The cells were maintained at 37 °C in a 5% CO_2 atmosphere. C2-ceramide (N-ethanoyl-D-erythro-sphingosine), C16-ceramide (N-palmitoyl-D-erythro-sphingosine) and C18-ceramide (N-stearoyl-D-erythro-sphingosine) were obtained from Acros Organics (345210500, 331540050, and 331550050, respectively). C8-ceramide (N-octanoyl-D-erythro-sphingosine) was from BIOMOL (BML-SL112-0005) and C2DHC (C2-dihydroceramide) from Sigma-Aldrich (E7980). All ceramides were dissolved in ethanol. To allow the entrance of long-chain ceramide in the cell, dodecan (Filter Service, 117590250) was added to the medium (0.02%). For all experiments, an equal amount of solvent (ethanol/dodecan) was added to control cultures (i.e., untreated cells) compared with the corresponding ceramide-treated conditions. λ Protein Phosphatase (λ-PPase) was purchased from New England BioLabs (P0753S), staurosporine from Sigma-Aldrich (S4400) and H-89 dihydrochloride from Calbiochem (371963).

Protein extraction and western blot analysis

HCT116 cells were scraped and centrifuged at 1000 g for 5 min. The pellets were washed 2 times with ice-cold PBS (Lonza, BE17-516F). Protein extracts were prepared by lysing the cells in 1% sodium dodecyl sulfate (SDS; Sigma Aldrich, L3771). The cells were vortexed and protein extracts were obtained after 10 min boiling. Protein concentrations were measured using the Micro BCA protein assay reagent kit (Pierce, 23225). Proteins were separated by SDS-PAGE and transferred to polyvinylidene difluoride membranes (Millipore, IPVH00010). After blocking, the membranes were incubated with the monoclonal anti-EMD antibody (Santa Cruz, sc-25284). The anti-MAP1LC3B (3868), anti-AKT1 (2966), anti-p-AKT1 (4058), anti-MTOR (2983), anti-p-MTOR (2971), anti-RPS6KB1 (9202) and anti-p-RPS6KB1 (9234) antibodies were purchased from Cell Signaling Technology. The anti-TUBA1A (T6074) and the anti-FLAG (F7425) antibodies were from Sigma-Aldrich. The membranes were incubated with 1:10000 diluted peroxidase-conjugated anti-mouse (NA931) and

anti-rabbit (NA934) secondary antibodies (GE Healthcare). The reactions were revealed with the enhanced chemiluminescence detection reagent (ECL kit, Thermo Scientific, 32106). When required, the detected signals were analyzed by densitometry. The intensity of each band was measured with the Imagequant TL software (GE Healthcare). To normalize protein levels, the value of the band corresponding to each protein level was normalized with the intensity of the corresponding anti-TUBA1A signal used as an internal standard. Statistical analysis was performed by the Student *t* test using Prism 4.00 software (Graph pad), with statistical significance accepted at $P < 0.05$.

Phosphatase and kinase inhibitor assays

HCT116 cells were scraped, centrifuged at 1000 g for 5 min. The pellets were washed 2 times with ice-cold PBS. Cytosolic protein extracts were prepared by lysing the cells in the following buffer: 25 mM HEPES (Sigma Aldrich, H3375), 150 mM NaCl, 0.5% Triton X-100 (Acros Organics, 9002-93-1), 10% glycerol, 1 mM dithiothreitol, 25 mM glycerophosphate (Sigma Aldrich, G-5422), 1 mM sodium orthovanadate (Sigma Aldrich, 450-243), 1 mM sodium fluorure (Sigma Aldrich, S7920) containing a cocktail of protease inhibitors (Complete™, Roche, 11836145001). The cells were vortexed and kept on ice for 5 min. Protein extract was obtained after 15 min centrifugation (4 °C) at 16,100 g. Five microliters of phosphatase buffer (50 mM TRIS-HCl, 100 mM NaCl, 2 mM DTT, 0.1 mM EDTA and 0.01% Brij 35 [Sigma Aldrich, 858366]) was added to 50 μl of lysate, followed by incubation with 2 mM $MnCl_2$ and 1600 U of λ-PPase at 30 °C for 30 min. For the kinase inhibitor assays, HCT116 cells were pretreated with staurosporine (100 nM) for 30 min, protein kinase inhibitor (10 μM, 30 min; Calbiochem, 476485), Rp-8-Br-cAMP (250 μM, 30 min; Calbiochem, 116816), 8-CPT-cAMP (50 μM, 30 min; Calbiochem, 116812) or with H89 (5 μM; Calbiochem, 371963) for 1 h and left treated with or without C16-ceramide (12 μM) for 1, 3 or 6 h.

RNA interference

For RNA interference, decreased *EMD* or *ATG7* expression was obtained by transfecting ON-TARGETplus SMARTpool siRNA (Dharmacon, L-011025-00-0020 and L-020112-00-0005 respectively) using lipofectamine reagent according to the protocol provided by the manufacturer (Invitrogen, 11668-019). Colon cancer cells were seeded in 6-well plates and transfected with *GFP* siRNA or *EMD* siRNA and left untreated or treated with C16-ceramide (12 μM) for 1, 3, or 6 h. Cells were harvested 48 h after transfection.

Transient transfection

The ORF encoding human *EMD* was cloned into pIRESpuro vector (Clontech, 6031-1) containing a FLAG tag in the C terminus. *EMD* mutants (LEMΔ, N74Δ and N105Δ) were generated by PCR and subcloned into the pIRESpuro FLAG vector. HCT116 cells were seeded in 6-well plates and transfected with empty vector, EMD-FLAG or mutant expression vector using lipofectamine with a 1:2 DNA/lipofectamine ratio and left untreated or treated with C16-ceramide (12 μM) for 1, 3, or 6 h. Cells were harvested 24 h after transfection.

Generation of stable cell line

The lentiviral vectors were generated by cotransfecting Lenti-X 293T cells (Clontech, 632180) with a pSPAX2 (Addgene, 12260) and a VSV-G encoding vector (Emi N, Friedmann T, Yee JK (1991) along with a pLenti6-EMD-FLAG plasmid (EMD-FLAG sequence cloned into a modified pLenti6/V5 directional TOPO, Invitrogen, K49-55) or with a eGFP-V5 (eGFP sequence cloned into pLenti6/V5 directional TOPO, Invitrogen)-encoding plasmid. 48 h and 72 h h post transfection, viral supernatants were collected. HCT116 cells were then incubated with the lentiviral vectors for 24 h. After 48 h, the transduced cells were selected using Blasticidin (Sigma-Aldrich, 15205) at 0.1 mg/mL.

Immunofluorescence

HCT116 cells stably expressing EMD-FLAG or control vector or cells without transfection for the endogenous colocalization were plated on glass coverslips placed in 6-wells and treated with or without C16-ceramide (12 μM) for 3 h. Cells were fixed in 4% paraformaldehyde in PBS for 20 min, rinsed 3 times with PBS, and permeabilized with methanol for 10 min at –20 °C. The coverslips were then blocked in 5% goat serum and 0.3% triton in PBS for one h at room temperature. Cells were then labeled with an anti-MAP1LC3B antibody, 1/100 (Cell Signaling Technology, 3868) or with anti-EMD antibody (Santa Cruz, sc-25284) diluted in blocking buffer and incubated overnight at 4 °C. After 3 washes in PBS, antibody complexes were detected with Alexa Fluor 488 goat anti-rabbit antibody (Invitrogen, A11008) in a 1/500 dilution. Coverslips were mounted in Prolong (Invitrogen, P36930). Images were acquired by using a Confocal Leica TCS SP5 (Leica Microsystems, GIGA +4, Avenue de l'Hôpital, 1 (B34) 4000, Sart-Tilman, Belgique). Autophagosome formation was quantified by counting the percentage of cells presenting MAP1LC3B vacuoles. A minimum of 200 cells was considered for each analysis and experiments were made in triplicate. Statistical analysis was performed by the Student *t* test using Prism 4.00 software (Graph pad), with statistical significance accepted at $P < 0.05$.

Immunoprecipitation

Cells were transfected with EMD-FLAG vector or with empty vector as control and then treated with or without 12 μM of C16-ceramide for 3 h. Protein extracts were then incubated with FLAG beads (Sigma, F2426) under gentle agitation overnight at 4 °C. After 5 washes in lysis buffer, bound proteins were resolved by SDS-PAGE and analyzed by western blotting with an anti-MAP1LC3B antibody.

Disclosure of Potential Conflicts of Interest

No potential conflicts of interest were disclosed.

Acknowledgments

MP Merville is a senior research associate at the National Fund for Scientific Research (FR-FNRS), Belgium. This work was financially supported by ARC fund and Léon Frédéricq grant from University of Liège. We thank the "Imaging Platform" (S Ormenese and G Moraes, GIGA,

University of Liège) for the confocal imaging and the "Viral vector platform" (E Divalentin, GIGA, University of Liège) for stable cell lines generation.

Supplemental Materials

Supplemental materials may be found here:
www.landesbioscience.com/journals/autophagy/article/28777

References

1. Hannun YA. Functions of ceramide in coordinating cellular responses to stress. Science 1996; 274:1855-9; PMID:8943189; http://dx.doi.org/10.1126/science.274.5294.1855
2. Ogretmen B, Hannun YA. Biologically active sphingolipids in cancer pathogenesis and treatment. Nat Rev Cancer 2004; 4:604-16; PMID:15286740; http://dx.doi.org/10.1038/nrc1411
3. Morad SA, Cabot MC. Ceramide-orchestrated signalling in cancer cells. Nat Rev Cancer 2013; 13:51-65; PMID:23235911; http://dx.doi.org/10.1038/nrc3398
4. Obeid LM, Linardic CM, Karolak LA, Hannun YA. Programmed cell death induced by ceramide. Science 1993; 259:1769-71; PMID:8456305; http://dx.doi.org/10.1126/science.8456305
5. Pettus BJ, Chalfant CE, Hannun YA. Ceramide in apoptosis: an overview and current perspectives. Biochim Biophys Acta 2002; 1585:114-25; PMID:12531544; http://dx.doi.org/10.1016/S1388-1981(02)00331-1
6. Siskind LJ. Mitochondrial ceramide and the induction of apoptosis. J Bioenerg Biomembr 2005; 37:143-53; PMID:16167171; http://dx.doi.org/10.1007/s10863-005-6567-7
7. Mullen TD, Obeid LM. Ceramide and apoptosis: exploring the enigmatic connections between sphingolipid metabolism and programmed cell death. Anticancer Agents Med Chem 2012; 12:340-63; PMID:21707511; http://dx.doi.org/10.2174/187152012800228661
8. Lavieu G, Scarlatti F, Sala G, Levade T, Ghidoni R, Botti J, Codogno P. Is autophagy the key mechanism by which the sphingolipid rheostat controls the cell fate decision? Autophagy 2007; 3:45-7; PMID:17035732
9. Bedia C, Levade T, Codogno P. Regulation of autophagy by sphingolipids. Anticancer Agents Med Chem 2011; 11:844-53; PMID:21707487; http://dx.doi.org/10.2174/187152011797655131
10. Quan W, Lim YM, Lee MS. Role of autophagy in diabetes and endoplasmic reticulum stress of pancreatic β-cells. Exp Mol Med 2012; 44:81-8; PMID:22257883; http://dx.doi.org/10.3858/emm.2012.44.2.030
11. Sridhar S, Botbol Y, Macian F, Cuervo AM. Autophagy and disease: always two sides to a problem. J Pathol 2012; 226:255-73; PMID:21990109; http://dx.doi.org/10.1002/path.3025
12. Scarlatti F, Bauvy C, Ventruti A, Sala G, Cluzeaud F, Vandewalle A, Ghidoni R, Codogno P. Ceramide-mediated macroautophagy involves inhibition of protein kinase B and up-regulation of beclin 1. J Biol Chem 2004; 279:18384-91; PMID:14970205; http://dx.doi.org/10.1074/jbc.M313561200
13. Daido S, Kanzawa T, Yamamoto A, Takeuchi H, Kondo Y, Kondo S. Pivotal role of the cell death factor BNIP3 in ceramide-induced autophagic cell death in malignant glioma cells. Cancer Res 2004; 64:4286-93; PMID:15205343; http://dx.doi.org/10.1158/0008-5472.CAN-03-3084
14. Pattingre S, Bauvy C, Levade T, Levine B, Codogno P. Ceramide-induced autophagy: to junk or to protect cells? Autophagy 2009; 5:558-60; PMID:19337026; http://dx.doi.org/10.4161/auto.5.4.8390
15. Pattingre S, Bauvy C, Carpentier S, Levade T, Levine B, Codogno P. Role of JNK1-dependent Bcl-2 phosphorylation in ceramide-induced macroautophagy. J Biol Chem 2009; 284:2719-28; PMID:19029119; http://dx.doi.org/10.1074/jbc.M805920200
16. Spassieva SD, Mullen TD, Townsend DM, Obeid LM. Disruption of ceramide synthesis by CerS2 down-regulation leads to autophagy and the unfolded protein response. Biochem J 2009; 424:273-83; PMID:19728861; http://dx.doi.org/10.1042/BJ20090699
17. Sentelle RD, Senkal CE, Jiang W, Ponnusamy S, Gencer S, Selvam SP, Ramshesh VK, Peterson YK, Lemasters JJ, Szulc ZM, et al. Ceramide targets autophagosomes to mitochondria and induces lethal mitophagy. Nat Chem Biol 2012; 8:831-8; PMID:22922758; http://dx.doi.org/10.1038/nchembio.1059
18. Rénert AF, Leprince P, Dieu M, Renaut J, Raes M, Bours V, Chapelle JP, Piette J, Merville MP, Fillet M. The proapoptotic C16-ceramide-dependent pathway requires the death-promoting factor Btf in colon adenocarcinoma cells. J Proteome Res 2009; 8:4810-22; PMID:19705920; http://dx.doi.org/10.1021/pr9005316
19. Haraguchi T, Holaska JM, Yamane M, Koujin T, Hashiguchi N, Mori C, Wilson KL, Hiraoka Y. Emerin binding to Btf, a death-promoting transcriptional repressor, is disrupted by a missense mutation that causes Emery-Dreifuss muscular dystrophy. Eur J Biochem 2004; 271:1035-45; PMID:15009215; http://dx.doi.org/10.1111/j.1432-1033.2004.04007.x
20. Lin F, Blake DL, Callebaut I, Skerjanc IS, Holmer L, McBurney MW, Paulin-Levasseur M, Worman HJ. MAN1, an inner nuclear membrane protein that shares the LEM domain with lamina-associated polypeptide 2 and emerin. J Biol Chem 2000; 275:4840-7; PMID:10671519; http://dx.doi.org/10.1074/jbc.275.7.4840
21. Laguri C, Gilquin B, Wolff N, Romi-Lebrun R, Courchay K, Callebaut I, Worman HJ, Zinn-Justin S. Structural characterization of the LEM motif common to three human inner nuclear membrane proteins. Structure 2001; 9:503-11; PMID:11435115; http://dx.doi.org/10.1016/S0969-2126(01)00611-6
22. Haraguchi T, Koujin T, Segura-Totten M, Lee KK, Matsuoka Y, Yoneda Y, Wilson KL, Hiraoka Y. BAF is required for emerin assembly into the reforming nuclear envelope. J Cell Sci 2001; 114:4575-85; PMID:11792822
23. Lee KK, Haraguchi T, Lee RS, Koujin T, Hiraoka Y, Wilson KL. Distinct functional domains in emerin bind lamin A and DNA-bridging protein BAF. J Cell Sci 2001; 114:4567-73; PMID:11792821
24. Segura-Totten M, Kowalski AK, Craigie R, Wilson KL. Barrier-to-autointegration factor: major roles in chromatin decondensation and nuclear assembly. J Cell Biol 2002; 158:475-85; PMID:12163470; http://dx.doi.org/10.1083/jcb.200202019
25. Furukawa K, Sugiyama S, Osouda S, Goto H, Inagaki M, Horigome T, Omata S, McConnell M, Fisher PA, Nishida Y. Barrier-to-autointegration factor plays crucial roles in cell cycle progression and nuclear organization in Drosophila. J Cell Sci 2003; 116:3811-23; PMID:12902403; http://dx.doi.org/10.1242/jcs.00682
26. Margalit A, Vlcek S, Gruenbaum Y, Foisner R. Breaking and making of the nuclear envelope. J Cell Biochem 2005; 95:454-65; PMID:15832341; http://dx.doi.org/10.1002/jcb.20433
27. Wang X, Xu S, Rivolta C, Li LY, Peng GH, Swain PK, Sung CH, Swaroop A, Berson EL, Dryja TP, et al. Barrier to autointegration factor interacts with the cone-rod homeobox and represses its transactivation function. J Biol Chem 2002; 277:43288-300; PMID:12215455; http://dx.doi.org/10.1074/jbc.M207952200
28. Holaska JM, Lee KK, Kowalski AK, Wilson KL. Transcriptional repressor germ cell-less (GCL) and barrier to autointegration factor (BAF) compete for binding to emerin in vitro. J Biol Chem 2003; 278:6969-75; PMID:12493765; http://dx.doi.org/10.1074/jbc.M208811200
29. Fairley EA, Kendrick-Jones J, Ellis JA. The Emery-Dreifuss muscular dystrophy phenotype arises from aberrant targeting and binding of emerin at the inner nuclear membrane. J Cell Sci 1999; 112:2571-82; PMID:10393813
30. Clements L, Manilal S, Love DR, Morris GE. Direct interaction between emerin and lamin A. Biochem Biophys Res Commun 2000; 267:709-14; PMID:10673356; http://dx.doi.org/10.1006/bbrc.1999.2023
31. Holaska JM, Wilson KL. An emerin "proteome": purification of distinct emerin-containing complexes from HeLa cells suggests molecular basis for diverse roles including gene regulation, mRNA splicing, signaling, mechanosensing, and nuclear architecture. Biochemistry 2007; 46:8897-908; PMID:17620012; http://dx.doi.org/10.1021/bi602636m
32. Demmerle J, Koch AJ, Holaska JM. The nuclear envelope protein emerin binds directly to histone deacetylase 3 (HDAC3) and activates HDAC3 activity. J Biol Chem 2012; 287:22080-8; PMID:22570481; http://dx.doi.org/10.1074/jbc.M111.325308
33. Muchir A, Pavlidis P, Bonne G, Hayashi YK, Worman HJ. Activation of MAPK in hearts of EMD null mice: similarities between mouse models of X-linked and autosomal dominant Emery Dreifuss muscular dystrophy. Hum Mol Genet 2007; 16:1884-95; PMID:17567779; http://dx.doi.org/10.1093/hmg/ddm137
34. Muchir A, Pavlidis P, Decostre V, Herron AJ, Arimura T, Bonne G, Worman HJ. Activation of MAPK pathways links LMNA mutations to cardiomyopathy in Emery-Dreifuss muscular dystrophy. J Clin Invest 2007; 117:1282-93; PMID:17446932; http://dx.doi.org/10.1172/JCI29042
35. Ellis JA, Craxton M, Yates JR, Kendrick-Jones J. Aberrant intracellular targeting and cell cycle-dependent phosphorylation of emerin contribute to the Emery-Dreifuss muscular dystrophy phenotype. J Cell Sci 1998; 111:781-92; PMID:9472006
36. Hirano Y, Segawa M, Ouchi FS, Yamakawa Y, Furukawa K, Takeyasu K, Horigome T. Dissociation of emerin from barrier-to-autointegration factor is regulated through mitotic phosphorylation of emerin in a xenopus egg cell-free system. J Biol Chem 2005; 280:39925-33; PMID:16204256; http://dx.doi.org/10.1074/jbc.M503214200
37. Roberts RC, Sutherland-Smith AJ, Wheeler MA, Jensen ON, Emerson LJ, Spiliotis II, Tate CG, Kendrick-Jones J, Ellis JA. The Emery-Dreifuss muscular dystrophy associated-protein emerin is phosphorylated on serine 49 by protein kinase A. FEBS J 2006; 273:4562-75; PMID:16972941; http://dx.doi.org/10.1111/j.1742-4658.2006.05464.x
38. Rush J, Moritz A, Lee KA, Guo A, Goss VL, Spek EJ, Zhang H, Zha XM, Polakiewicz RD, Comb MJ. Immunoaffinity profiling of tyrosine phosphorylation in cancer cells. Nat Biotechnol 2005; 23:94-101; PMID:15592455; http://dx.doi.org/10.1038/nbt1046
39. Olsen JV, Blagoev B, Gnad F, Macek B, Kumar C, Mortensen P, Mann M. Global, in vivo, and site-specific phosphorylation dynamics in signaling networks. Cell 2006; 127:635-48; PMID:17081983; http://dx.doi.org/10.1016/j.cell.2006.09.026

40. Schlosser A, Amanchy R, Otto H. Identification of tyrosine-phosphorylation sites in the nuclear membrane protein emerin. FEBS J 2006; 273:3204-15; PMID:16857009; http://dx.doi.org/10.1111/j.1742-4658.2006.05329.x
41. Tifft KE, Bradbury KA, Wilson KL. Tyrosine phosphorylation of nuclear-membrane protein emerin by Src, Abl and other kinases. J Cell Sci 2009; 122:3780-90; PMID:19789182; http://dx.doi.org/10.1242/jcs.048397
42. Yip SC, Cotteret S, Chernoff J. Sumoylated protein tyrosine phosphatase 1B localizes to the inner nuclear membrane and regulates the tyrosine phosphorylation of emerin. J Cell Sci 2012; 125:310-6; PMID:22266903; http://dx.doi.org/10.1242/jcs.086256
43. Morris JB, Hofemeister H, O'Hare P. Herpes simplex virus infection induces phosphorylation and delocalization of emerin, a key inner nuclear membrane protein. J Virol 2007; 81:4429-37; PMID:17301149; http://dx.doi.org/10.1128/JVI.02354-06
44. Leach N, Bjerke SL, Christensen DK, Bouchard JM, Mou F, Park R, Baines J, Haraguchi T, Roller RJ. Emerin is hyperphosphorylated and redistributed in herpes simplex virus type 1-infected cells in a manner dependent on both UL34 and US3. J Virol 2007; 81:10792-803; PMID:17652388; http://dx.doi.org/10.1128/JVI.00196-07
45. Jayadev S, Liu B, Bielawska AE, Lee JY, Nazaire F, Pushkareva MYu, Obeid LM, Hannun YA. Role for ceramide in cell cycle arrest. J Biol Chem 1995; 270:2047-52; PMID:7836432; http://dx.doi.org/10.1074/jbc.270.5.2047
46. Bandyopadhyay U, Cuervo AM. Chaperone-mediated autophagy in aging and neurodegeneration: lessons from alpha-synuclein. Exp Gerontol 2007; 42:120-8; PMID:16860504; http://dx.doi.org/10.1016/j.exger.2006.05.019
47. Mizushima N. Autophagy: process and function. Genes Dev 2007; 21:2861-73; PMID:18006683; http://dx.doi.org/10.1101/gad.1599207
48. Wilkinson FL, Holaska JM, Zhang Z, Sharma A, Manilal S, Holt I, Stamm S, Wilson KL, Morris GE. Emerin interacts in vitro with the splicing-associated factor, YT521-B. Eur J Biochem 2003; 270:2459-66; PMID:12755701; http://dx.doi.org/10.1046/j.1432-1033.2003.03617.x
49. Holaska JM, Kowalski AK, Wilson KL. Emerin caps the pointed end of actin filaments: evidence for an actin cortical network at the nuclear inner membrane. PLoS Biol 2004; 2:E231; PMID:15328537; http://dx.doi.org/10.1371/journal.pbio.0020231
50. Daub H, Olsen JV, Bairlein M, Gnad F, Oppermann FS, Körner R, Greff Z, Kéri G, Stemmann O, Mann M. Kinase-selective enrichment enables quantitative phosphoproteomics of the kinome across the cell cycle. Mol Cell 2008; 31:438-48; PMID:18691976; http://dx.doi.org/10.1016/j.molcel.2008.07.007
51. Pan C, Gnad F, Olsen JV, Mann M. Quantitative phosphoproteome analysis of a mouse liver cell line reveals specificity of phosphatase inhibitors. Proteomics 2008; 8:4534-46; PMID:18846507; http://dx.doi.org/10.1002/pmic.200800105
52. Amanchy R, Kalume DE, Iwahori A, Zhong J, Pandey A. Phosphoproteome analysis of HeLa cells using stable isotope labeling with amino acids in cell culture (SILAC). J Proteome Res 2005; 4:1661-71; PMID:16212419; http://dx.doi.org/10.1021/pr050134h
53. Dbaibo GS. Regulation of the stress response by ceramide. Biochem Soc Trans 1997; 25:557-61; PMID:9191155
54. Plo I, Ghandour S, Feutz AC, Clanet M, Laurent G, Bettaieb A. Involvement of de novo ceramide biosynthesis in lymphotoxin-induced oligodendrocyte death. Neuroreport 1999; 10:2373-6; PMID:10439466; http://dx.doi.org/10.1097/00001756-199908020-00028
55. Levy JM, Thorburn A. Targeting autophagy during cancer therapy to improve clinical outcomes. Pharmacol Ther 2011; 131:130-41; PMID:21440002; http://dx.doi.org/10.1016/j.pharmthera.2011.03.009
56. Hu YL, Jahangiri A, Delay M, Aghi MK. Tumor cell autophagy as an adaptive response mediating resistance to treatments such as antiangiogenic therapy. Cancer Res 2012; 72:4294-9; PMID:22915758; http://dx.doi.org/10.1158/0008-5472.CAN-12-1076
57. Palumbo S, Comincini S. Autophagy and ionizing radiation in tumors: the "survive or not survive" dilemma. J Cell Physiol 2013; 228:1-8; PMID:22585676; http://dx.doi.org/10.1002/jcp.24118
58. Koukourakis MI, Giatromanolaki A, Sivridis E, Pitiakoudis M, Gatter KC, Harris AL. Beclin 1 over- and underexpression in colorectal cancer: distinct patterns relate to prognosis and tumour hypoxia. Br J Cancer 2010; 103:1209-14; PMID:20842118; http://dx.doi.org/10.1038/sj.bjc.6605904
59. Bianco R, Garofalo S, Rosa R, Damiano V, Gelardi T, Daniele G, Marciano R, Ciardiello F, Tortora G. Inhibition of mTOR pathway by everolimus cooperates with EGFR inhibitors in human tumours sensitive and resistant to anti-EGFR drugs. Br J Cancer 2008; 98:923-30; PMID:18319715; http://dx.doi.org/10.1038/sj.bjc.6604269
60. Park MA, Zhang G, Norris J, Hylemon PB, Fisher PB, Grant S, Dent P. Regulation of autophagy by ceramide-CD95-PERK signaling. Autophagy 2008; 4:929-31; PMID:18719356
61. Yacoub A, Hamed HA, Allegood J, Mitchell C, Spiegel S, Lesniak MS, Ogretmen B, Dash R, Sarkar D, Broaddus WC, et al. PERK-dependent regulation of ceramide synthase 6 and thioredoxin play a key role in mda-7/IL-24-induced killing of primary human glioblastoma multiforme cells. Cancer Res 2010; 70:1120-9; PMID:20103619; http://dx.doi.org/10.1158/0008-5472.CAN-09-4043
62. Bhutia SK, Dash R, Das SK, Azab B, Su ZZ, Lee SG, Grant S, Yacoub A, Dent P, Curiel DT, et al. Mechanism of autophagy to apoptosis switch triggered in prostate cancer cells by antitumor cytokine melanoma differentiation-associated gene 7/interleukin-24. Cancer Res 2010; 70:3667-76; PMID:20406981; http://dx.doi.org/10.1158/0008-5472.CAN-09-3647
63. Ito H, Murakami M, Furuhata A, Gao S, Yoshida K, Sobue S, Hagiwara K, Takagi A, Kojima T, Suzuki M, et al. Transcriptional regulation of neutral sphingomyelinase 2 gene expression of a human breast cancer cell line, MCF-7, induced by the anti-cancer drug, daunorubicin. Biochim Biophys Acta 2009; 1789:681-90; PMID:19698806; http://dx.doi.org/10.1016/j.bbagrm.2009.08.006
64. Olshefski RS, Ladisch S. Glucosylceramide synthase inhibition enhances vincristine-induced cytotoxicity. Int J Cancer 2001; 93:131-8; PMID:11391632; http://dx.doi.org/10.1002/ijc.1301
65. Guenther GG, Peralta ER, Rosales KR, Wong SY, Siskind LJ, Edinger AL. Ceramide starves cells to death by downregulating nutrient transporter proteins. Proc Natl Acad Sci U S A 2008; 105:17402-7; PMID:18981422; http://dx.doi.org/10.1073/pnas.0802781105
66. Park YE, Hayashi YK, Bonne G, Arimura T, Noguchi S, Nonaka I, Nishino I. Autophagic degradation of nuclear components in mammalian cells. Autophagy 2009; 5:795-804; PMID:19550147